

A Cost-Effective Cyber-Defense Strategy: Attack-Induced Region Minimization and Cybersecurity Margin Maximization

Jiazuo Hou, *Graduate Student Member, IEEE*, Fei Teng, *Senior Member, IEEE*

Wenqian Yin, *Graduate Student Member, IEEE*, Yue Song, *Member, IEEE*, and Yunhe Hou, *Senior Member, IEEE*

Abstract—Recent years have witnessed increasing cyber-attack reports, e.g., the false data injection (FDI) cyber-attacks, which result in massive damage to power systems. This paper proposes a cost-effective two-stage cyber-defense strategy, which minimizes the FDI attack-induced region in the system planning stage, followed by the cybersecurity margin maximization in the system operation stage. First, this paper proposes a shaping cyber-defense strategy that achieves a balance between shaping the FDI attack-induced region and minimizing the cyber-defense meters. The proposed shaping cyber-defense strategy is formulated as a one-leader-multi-follower bi-level problem, which is converted into a single-level mixed-integer linear programming (MILP) problem with closed-form lower bounds of the big-M. Then, via optimal dispatch of operation points, this paper proposes a dispatching cyber-defense strategy, which achieves a trade-off between maximizing the cybersecurity margin and minimizing the additional operation cost. This leads to a balance between the safest-but-expensive operation point (i.e., Euclidean Chebyshev center) and the cheapest-but-dangerous operation point. Simulation results on a modified IEEE 14 bus system verify the effectiveness and cost-effectiveness of the proposed shape-and-dispatch cyber-defense strategy.

Index Terms—Attack-Induced region, cyber-defense cost-benefit trade-off, cybersecurity margin, Euclidean Chebyshev center, false data injection cyber-attack, security region.

NOMENCLATURE

System Variable

D, G, F	load, generation, and line flow vector
$\underline{G}, \overline{G}$	lower and upper limits of generation vector
\overline{F}	upper limits of line flow vector
S	shifting factor matrix, whose n -th row vector is S_n
U_G, U_D	bus-generator incidence matrix and bus-load incidence matrix
\mathcal{D}, \mathcal{L}	set of all loads and all lines
D, L, P	number of loads, lines, and buses
c	generation cost vector
Θ^{security}	security region
$\Theta^{\text{insecurity}}$	insecurity region

Cyber-Attack Variable

Jiazuo Hou, Wenqian Yin, Yue Song, and Yunhe Hou are with the Department of Electrical and Electronic Engineering, The University of Hong Kong, Hong Kong SAR, China; Jiazuo Hou and Yunhe Hou are also with The University of Hong Kong Shenzhen Institute of Research and Innovation, Shenzhen 518057, China (e-mail: jzhou@eee.hku.hk, wqyin@eee.hku.hk, yuesong@eee.hku.hk, yhhou@eee.hku.hk).

Fei Teng is with the Department of Electrical and Electronic Engineering, Imperial College London, SW7 2AZ London, U.K. (e-mail: f.teng@imperial.ac.uk).

$\Delta D = \{\Delta D_d\}$	FDI attack injection on the d -th load measurement
$\Delta F = \{\Delta F_n\}$	FDI attack injection on the n -th line flow measurement
ΔD^n	FDI attack injection vector with respect to the n -th line
$\tau = \{\tau_d\}$	FDI attacking ability on the d -th load measurement
$H = \{H_n\}$	maximum line overloading of the n -th line
$V = \{V_n\}$	minimum line overloading of the n -th line
Ω^{ARR}	FDI attack-reachable region (ARR)
Ω^{AIR}	FDI attack-induced region (AIR)
Γ^{security}	preventive security region

Cyber-Defense Variable

$\delta = \{\delta_d\}$	cyber-defense meter placement state (binary variable) of the d -th load measurement
$\varepsilon = \{\varepsilon_n\}$	cyber-defense meter placement state (binary variable) of the n -th line flow measurement
$B^{\text{AIR}}, C^{\text{AIR}}$	cyber-defense benefit and cost of the proposed shaping cyber-defense strategy
$\omega^{\text{AIR}}, \overline{C^{\text{AIR}}}$	cyber-defense cost coefficient and cost budget of the proposed shaping cyber-defense strategy
B^G, C^G	cyber-defense benefit and cost of the proposed dispatching cyber-defense strategy
ω^G	cyber-defense cost coefficient of the proposed dispatching cyber-defense strategy
$r(G)$	cybersecurity margin of operation point G
λ^n	Lagrange multiplier associated with the power balance equation of the n -th line-oriented FDI attack
$\underline{\alpha}^n, \overline{\alpha}^n$	Lagrange multiplier vectors associated with the load injection limits of the n -th line-oriented FDI attack
$\underline{\beta}^n, \overline{\beta}^n$	Lagrange multiplier vectors associated with the line injection limits of the n -th line-oriented FDI attack
$u_{\underline{\alpha}^n}, u_{\overline{\alpha}^n}$	additional binary vector regarding the complementary slackness conditions of $\underline{\alpha}^n$ and $\overline{\alpha}^n$
$u_{\underline{\beta}^n}, u_{\overline{\beta}^n}$	additional binary vector regarding the complementary slackness conditions of $\underline{\beta}^n$ and $\overline{\beta}^n$
M, N, K	sufficiently large positive constants

I. INTRODUCTION

RECENT years have witnessed increasing reports on cyber-attack events [1], resulting in massive damage to power systems [2]. Therein, the false data injection (FDI) cyber-attack [3] is widely investigated in power systems [4], [5] due to its stealthiness, i.e., the ability to bypass the bad data detection (e.g., the largest normalized residual test [6]).

On the premise of stealthiness, the FDI cyber-attack has been demonstrated to achieve various attacking purposes, including but not limited to the economic loss [7], the stability deterioration [8], and more importantly, the line overloading [9], [10] that could result in not only instant line tripping but also subsequent cascading failure and even blackout.

Then, a follow-up question for both cyber attackers and cyber defenders is the *FDI capability boundary*, i.e., the *worst damaging impact* with respect to certain attacking purposes. The pioneering work [11] identifies the largest operation cost caused by the FDI cyber-attack. Che *et al.* investigate the worst line overloading [12]. Liu *et al.* find the most stealthy FDI with respect to learning-based detection [13]. Hou *et al.* address the most damaging effects on the small-signal stability margin [8].

In other words, within the FDI capability boundary, there exists an *FDI attack-induced region* with multiple feasible (i.e., stealthy) FDI solutions. In this regard, the power system cybersecurity is influenced by the FDI attack-induced region in two folds. First, the *volume* of the FDI attack-induced region indicates how many feasible FDI solutions exist. In this sense, minimizing the region volume could enhance the power system cybersecurity. Second, the minimum distance from an operation point to the region boundaries indicates the *cybersecurity margin* of the operation point. In this sense, a larger distance implies better power system cyber resilience.

Therefore, to enhance cybersecurity with respect to the FDI attack-induced region in both system planning and system operation, two successive intriguing questions arise:

- *Shaping region boundaries in system planning*: How to quantify the volume of the FDI attack-induced region? With limited cyber-defense meter resources in system planning stage, how to minimize the region volume by strategically shaping the region boundaries?
- *Dispatching operation points in system operation*: Given an FDI attack-induced region, how to quantify the cybersecurity margin of a certain operation point? With optimal dispatch of operation points in system operation stage, how to maximize the cybersecurity margin?

More importantly, due to the limited cyber-defense resources [14], it is important to address the cyber-defense strategies in a not only effective but also economic manner [15]. In this regard, the intriguing questions regarding how much the proposed cyber-defense strategy pays and gains [16] should be addressed:

- *Cyber-defense cost-benefit trade-off*: What are the cyber-defense costs to achieve the shape-and-dispatch cyber-defense strategy? How to balance the cyber-defense costs and benefits in both system planning and operation stages, leading to a cost-benefit trade-off?

Motivated by the above questions, this paper proposes a cost-effective shape-and-dispatch cyber-defense strategy, which minimizes the FDI attack-induced region in the system planning stage, followed by the cybersecurity margin maximization in the system operation stage. The contributions of this paper are summarized as follows.

- 1) This paper proposes a cost-effective shaping cyber-defense strategy, which achieves a trade-off between limiting the FDI attack-induced region and minimizing the cyber-defense meters via optimal meter placement. In particular, a sufficient condition for identifying the FDI unattackable lines is proposed.
- 2) The proposed shaping cyber-defense strategy is mathematically formulated as a one-leader-multi-follower bi-level problem, which is converted into a single-level mixed-integer linear programming (MILP) problem. Moreover, the closed-form lower bounds for three big-M constants are investigated.
- 3) Based on the preventive security region obtained from the proposed shaping cyber-defense strategy, this paper proposes a cost-effective dispatching cyber-defense strategy. With the optimal dispatch of operation points, the proposed strategy achieves a trade-off between maximizing the cybersecurity margin and minimizing the additional operation cost. This leads to a balance between the safest-but-expensive operation point (i.e., Euclidean Chebyshev center) and the cheapest-but-dangerous operation point.

The remaining of this paper is organized as follows. Section II illustrates the preliminaries of the FDI cyber-attack. Section III proposes a shaping cyber-defense strategy to limit the FDI attack-induced region in a cost-effective manner. Section IV reformulates the proposed shaping cyber-defense strategy into a single-level MILP problem. Section V proposes a cost-effective dispatching cyber-defense strategy to maximize the cybersecurity margin in a preventive security region. Section VI verifies the effectiveness and cost-effectiveness of the proposed shape-and-dispatch cyber-defense strategy. Section VII concludes this paper.

II. PRELIMINARIES OF THE FALSE DATA INJECTION CYBER-ATTACK

Consider a general optimal power flow (OPF) problem [17] that is subjected to the power balance (1), the generation limits (2), and the power flow equation and limits (3):

$$\mathbf{1}^T \mathbf{D} = \mathbf{1}^T \mathbf{G} \quad (1)$$

$$\underline{\mathbf{G}} \leq \mathbf{G} \leq \overline{\mathbf{G}} \quad (2)$$

$$-\overline{\mathbf{F}} \leq \mathbf{F} = \mathbf{S}(\mathbf{U}_G \mathbf{G} - \mathbf{U}_D \mathbf{D}) \leq \overline{\mathbf{F}} \quad (3)$$

where \mathbf{F} , \mathbf{D} , and \mathbf{G} are the line flow vector, the load vector, and the generation vector, respectively. \mathbf{S} is the shifting factor matrix. \mathbf{U}_G and \mathbf{U}_D are the bus-generator and bus-load incidence matrix, respectively. T represents transpose operation. $\overline{\mathbf{F}} > 0$ represents the line upper limits. $\overline{\mathbf{G}} > 0$ and $\underline{\mathbf{G}} \geq 0$ represent the generator upper and lower limits, respectively.

Assume the generation measurement is not easy to be attacked [11], leading to $\Delta \mathbf{G} = 0$, then we have the widely demonstrated fact.

Fact 1. (Stealthiness of FDI Cyber-Attack) The FDI cyber-attack [3] is able to bypass the bad data detection (i.e., the largest normalized residual test [6]) of power system state estimation and thus achieve the stealthiness, if the following conditions hold [11]:

- 1) the load measurement injection $\Delta \mathbf{D} = \{\Delta D_d\}$ satisfy the power balance (4) and the injection limitation (5);
- 2) the line flow measurement injection $\Delta \mathbf{F}$ satisfy the power flow equation and limits (6).

$$\mathbf{1}^T \Delta \mathbf{D} = 0 \quad (4)$$

$$-\delta \circ \tau \circ \mathbf{D} \leq \Delta \mathbf{D} \leq \delta \circ \tau \circ \mathbf{D} \quad (5)$$

$$-M\epsilon \leq \Delta \mathbf{F} = \mathbf{S} \mathbf{U}_D \Delta \mathbf{D} \leq M\epsilon \quad (6)$$

where \circ denotes the element-wise product. M is a sufficiently large constant. $\tau_d \in \tau$ represents the FDI attacking ability on the d -th load measurement.

$\delta = \{\delta_d\}$ and $\epsilon = \{\epsilon_n\}$ are binary variables. $\delta_d = 1$ (or $\epsilon_n = 1$) represents that the d -th load (or the n -th line flow) is not equipped with a cyber-defense load meter (or line meter), indicating that it could be possibly tampered by the FDI cyber-attack. Note that the cyber-defense resources, e.g., the cyber-defense meters, are usually limited [14] and thus should be optimally placed in the system planning stage.

By performing the stealthy FDI cyber-attack (4)-(6), the consequent line and load measurement are maliciously and stealthily altered, yielding

$$-\bar{\mathbf{F}} \leq \mathbf{S}(\mathbf{U}_G \mathbf{G} - \mathbf{U}_D(\mathbf{D} + \Delta \mathbf{D})) \leq \bar{\mathbf{F}} \quad (7)$$

As a result, the compromised power system OPF is misled and thus gives inappropriate generation dispatch \mathbf{G} . Since this paper focuses on the FDI attack-induced line overloading, the attacking objectives are the maximum and minimum overloading of each line (e.g., the n -th line), yielding the bi-level line overloading-oriented FDI cyber-attack [12]:

$$H_n/V_n = \max / \min \mathbf{S}_n \mathbf{U}_D \Delta \mathbf{D} \quad (8)$$

$$\begin{aligned} &\text{over } \Delta \mathbf{D} \in \mathbb{R}^D \\ &\text{s.t. (4), (5), (6)} \end{aligned}$$

where \mathbf{S}_n represents the n -th row vector of \mathbf{S} .

III. MINIMIZING THE FDI ATTACK-INDUCED REGION VIA A SHAPING CYBER-DEFENSE STRATEGY

To quantify and minimize the volume of the FDI attack-induced region, this section proposes a cost-effective shaping cyber-defense strategy, which is achieved by optimal cyber-defense meter placement in the system planning stage.

A. Definition and Geometric Illustration of Regions

Several regions that are defined in the generation injection space, i.e., \mathbf{G} space, are given as follows.

Definition 1. (Security and Insecurity Region) The security region Θ^{security} [18] and insecurity region $\Theta^{\text{insecurity}}$ of a power system are defined as:

$$\Theta^{\text{security}} := \{\mathbf{G} \mid (1), (2), (3)\} \quad (9)$$

$$\Theta^{\text{insecurity}} := \{\mathbf{G} \mid (1)\} \setminus \Theta^{\text{security}} \quad (10)$$

Note that \mathbf{V} and \mathbf{H} solved by (8) indicate the worst line overloading, i.e., the damaging boundary, of the stealthy FDI cyber-attack (4)-(6). That is, the stealthy FDI cyber-attack is able to cause any magnitude of line overloading within the damaging boundary \mathbf{V} and \mathbf{H} .

Thus, the lower and upper bounds of the line flow \mathbf{F} , i.e., $-\bar{\mathbf{F}}$ and $\bar{\mathbf{F}}$, are maliciously and stealthily expanded by \mathbf{V} and \mathbf{H} , respectively. This yields

$$\mathbf{V} - \bar{\mathbf{F}} \leq \mathbf{F} = \mathbf{S}(\mathbf{U}_G \mathbf{G} - \mathbf{U}_D \mathbf{D}) \leq \mathbf{H} + \bar{\mathbf{F}} \quad (11)$$

As a result, the line flow constraints (3) are violated if the consequent line flow \mathbf{F} fall in the following range:

$$\mathbf{V} - \bar{\mathbf{F}} \leq \mathbf{F} \leq -\bar{\mathbf{F}} \quad \text{or} \quad \bar{\mathbf{F}} \leq \mathbf{F} \leq \mathbf{H} + \bar{\mathbf{F}} \quad (12)$$

Then we have the following two regions related to the stealthy FDI cyber-attacks.

Definition 2. (FDI Attack-Induced Region) Consider a power system subjected to (1)-(3) is under stealthy FDI cyber-attack (4)-(6), the FDI attack-reachable region (ARR) Ω^{ARR} and the attack-induced region (AIR) Ω^{AIR} are defined as:

$$\Omega^{\text{ARR}} := \{\mathbf{G} \mid (1), (2), (11)\} \quad (13)$$

$$\Omega^{\text{AIR}} := \{\mathbf{G} \mid (1), (2), (12)\} \subset \Omega^{\text{ARR}} \quad (14)$$

According to the definitions, Ω^{ARR} in (9) and Θ^{security} in (13) are both polytopes in \mathbf{G} space. Thus, the aforementioned regions of a three-generator power system (with two independent generators) are conceptually illustrated in Fig. 1.

B. FDI Unattackable Lines

To start with, we have the following proposition for the maximum and minimum FDI attack-induced line overloading.

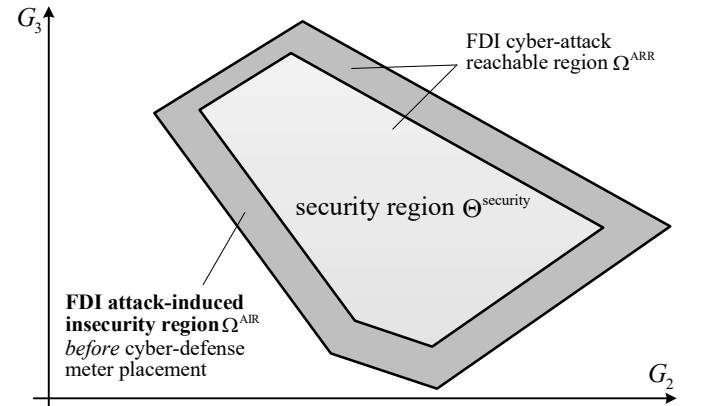


Fig. 1. Conceptual illustration of the security region Θ^{security} , the FDI attack-reachable region (ARR) Ω^{ARR} , and the FDI attack-induced region (AIR) Ω^{AIR} of a three-generator power system in \mathbf{G} space

Proposition 1. (Maximum and Minimum FDI Attack-Induced Line Overloading) \mathbf{H} and \mathbf{V} solved by (8) satisfy the following two properties:

$$\mathbf{H} = -\mathbf{V} \quad (15)$$

$$\mathbf{H} \geq 0, \mathbf{V} \leq 0 \quad (16)$$

Proof. $H_n = \max \mathbf{S}_n \mathbf{U}_D \Delta \mathbf{D} = \min -\mathbf{S}_n \mathbf{U}_D \Delta \mathbf{D} = -V_n$, yielding (15). Then, $H_n \geq V_n$ and (15) yield (16). \square

If the equality in (16) holds, we have the FDI unattackable line that is defined as follows.

Definition 3. (FDI Unattackable Line) The n -th line is termed as FDI unattackable if there exists no non-zero stealthy FDI cyber-attack (8) on the n -th line. That is, for any $\Delta \mathbf{D}$ that satisfies (4) and (5), we have

$$H_n = V_n = 0 \quad (17)$$

In the presence of a cyber-defense meter placement strategy δ and ε , the n -th line is unattackable if it is protected by a line flow cyber-defense meter, i.e., $\varepsilon_n = 0$. This is a trivial sufficient condition for identifying FDI unattackable lines protected by cyber-defense meters.

Let d'_n and d''_n denote the two terminal buses of the n -th line. Let $\mathcal{N}_d, d \in \{d'_n, d''_n\}$, denotes the set of all adjacent lines of the n -th line via the terminal bus d . Then, a non-trivial sufficient condition is illustrated as follows.

Proposition 2. (A Sufficient Condition for Identifying FDI Unattackable Lines Protected by Cyber-Defense Meters) Given a cyber-defense meter placement strategy δ and ε , the n -th line is unattackable if there exists $d \in \{d', d''\}$ such that

$$\delta_d = 0 \quad (18)$$

and

$$\sum_{l \in \mathcal{N}_d} \varepsilon_l = 0 \text{ or } \mathcal{N}_d = \emptyset \quad (19)$$

hold.

Proof. See Appendix A.

C. Quantifying the Volume of the FDI Attack-Induced Region

Proposition 1 indicates that Θ^{security} is a subset of Ω^{ARR} , yielding $\Omega^{\text{ARR}} \supseteq \Theta^{\text{security}}$. From a geometric viewpoint, Θ^{security} is similar to Ω^{ARR} in \mathbf{G} space in Fig. 1. Thus, the FDI attack-induced region Ω^{AIR} is the difference of the two polytopes, yielding

$$\Omega^{\text{AIR}} = \Omega^{\text{ARR}} \setminus \Theta^{\text{security}} = \Omega^{\text{ARR}} \cap \Theta^{\text{insecurity}} \quad (20)$$

Specifically, if all lines are unattackable, i.e., $\mathbf{H} = \mathbf{V} = \mathbf{0}$, then Ω^{ARR} would shrink to Θ^{security} and thus Ω^{AIR} would be an empty set.

Considering the geometric properties, the volume of Ω^{AIR} in Fig. 1 could be equivalently quantified by

$$\sum_{n \in \mathcal{L}} H_n / \bar{F}_n \quad (21)$$

where \mathcal{L} denotes the set of all lines. H_n in (21) indicates how large Θ^{security} is maliciously expanded to Ω^{ARR} with respect to the n -th line. \bar{F}_n in (21) indicates the normalization weight for the n -th line, leading to the weighted sum of H_n in (21).

D. Shaping the FDI Attack-Induced Region via Cost-Effective Cyber-Defense Meter Placement Strategy

Given the system topology and parameters, the volume of the FDI attack-induced region is determined by two factors:

- the FDI cyber-attack abilities (i.e., τ), whose increment could increase \mathbf{H} and thus increase the region volume;
- the cyber-defense meters (i.e., δ and ε), whose increment and optimal placement could decrease \mathbf{H} and thus decrease the region volume. This is conceptually illustrated in Fig. 2.

Since a smaller FDI attack-induced region volume is beneficial for the power system, the cyber-defense benefit of the proposed shaping cyber-defense strategy can be defined as

$$B^{\text{AIR}} = - \sum_{n \in \mathcal{L}} H_n / \bar{F}_n \quad (22)$$

The cyber-defense cost can be quantified by the sum of all the cyber-defense meters in load measurement and line flow measurement:

$$C^{\text{AIR}} = \sum_{d \in \mathcal{D}} (1 - \delta_d) + \sum_{n \in \mathcal{L}} (1 - \varepsilon_n) \leq \bar{C}^{\text{AIR}} \quad (23)$$

where \bar{C}^{AIR} indicates the limited budget of the cyber-defense meter costs.

As shown in Fig. 2, the system operators aim to minimize the FDI attack-induced region volume via strategically allocating the limited cyber-defense meters, leading to a trade-off between cyber-defense cost and benefit. This yields a one-leader-multi-follower bi-level optimization problem (denoted as **P1**):

$$\mathbf{P1} : \min -B^{\text{AIR}} + \omega^{\text{AIR}} C^{\text{AIR}}$$

$$\text{over } \delta \in \{0, 1\}^D, \varepsilon \in \{0, 1\}^L$$

$$\text{s.t. (22), (23)}$$

$$H_n = \max \mathbf{S}_n \mathbf{U}_D \Delta \mathbf{D}^n \quad \forall n \in \mathcal{L}$$

$$\text{over } \Delta \mathbf{D}^n \in \mathbb{R}^D \quad \forall n \in \mathcal{L}$$

$$\mathbf{1}^T \Delta \mathbf{D}^n = 0 \quad (24)$$

$$-\delta \circ \tau \circ \mathbf{D} \leq \Delta \mathbf{D}^n \leq \delta \circ \tau \circ \mathbf{D} \quad (25)$$

$$-M\varepsilon \leq \mathbf{S} \mathbf{U}_D \Delta \mathbf{D}^n \leq M\varepsilon \quad (26)$$

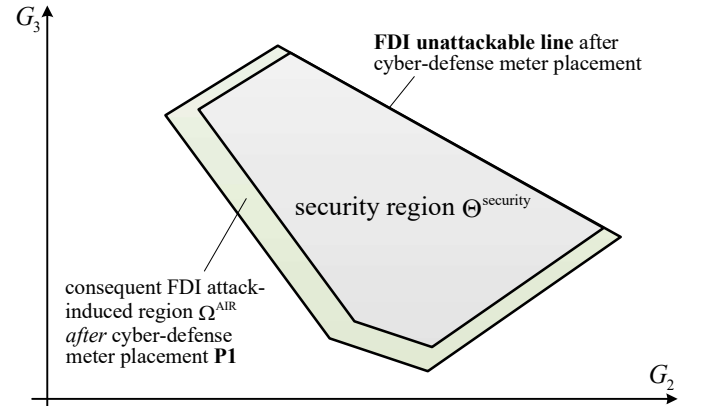


Fig. 2. Consequent FDI attack-induced region after implementing the proposed cyber-defense meter placement strategy **P1** on a three-generator power system

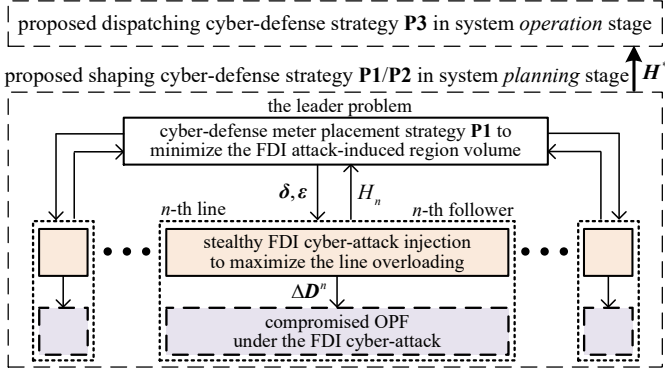


Fig. 3. Information transmission of the proposed shaping cyber-defense strategy **P1/P2** and the subsequent dispatching cyber-defense strategy **P3**

where ΔD^n denotes the FDI cyber-attack injections with respect to the n -th line. ω^{AIR} represents the weight coefficient to balance the cyber-defense cost and benefit.

The proposed one-leader-multi-follower bi-level problem **P1**, which will be converted into a single-level problem **P2** in Section IV, is intuitively illustrated in Fig. 3. The follower problem indicates the optimal FDI cyber-attack strategy for each line with a certain cyber-defense meter placement strategy, while the leader problem aims to find a cost-effective meter placement strategy with consideration of the maximum attack-induced line overloading of each line. After solving the proposed shaping cyber-defense strategy **P1/P2**, the consequent maximum line-overloading (denoted as H^*) will be delivered to the subsequent dispatching cyber-defense strategy **P3** in Section V.

IV. SOLUTION TO THE PROPOSED SHAPING CYBER-DEFENSE STRATEGY

To solve the proposed cost-effective cyber-defense meter placement strategy, which is a bi-level problem in **P1**, this section reformulates **P1** into a single-level MILP problem. Moreover, the closed-form lower bounds of the big-M are addressed to help efficiently solve the MILP problem.

A. Problem Reformulation

By applying the Karush-Kuhn-Tucker (KKT) optimality condition and the Fortuny-Amat mixed-integer reformulation [19], the original one-leader-multi-follower problem **P1** is converted into a single-level mixed-integer linear programming (MILP) problem (denoted as **P2**).

$$\begin{aligned} \mathbf{P2}: \min & B^{\text{AIR}} + \omega^{\text{AIR}} C^{\text{AIR}} \\ \text{over} & \delta \in \{0, 1\}^D, \epsilon \in \{0, 1\}^L \\ & \Delta D^n \in \mathbb{R}^D \quad \forall n \in \mathcal{L} \\ \text{s.t.} & (22), (23) \\ & (24), (25), (26) \quad \forall n \in \mathcal{L} \end{aligned} \quad (27)$$

$$H_n = S_n U_D \Delta D^n \quad \forall n \in \mathcal{L} \quad (28)$$

$$\begin{aligned} 0^T &= S_n U_D + \lambda^n \mathbf{1}^T + (\bar{\alpha}^n - \underline{\alpha}^n)^T \\ &+ (\bar{\beta}^n - \underline{\beta}^n)^T S U_D \end{aligned} \quad (29a)$$

$$\lambda^n \in \mathbb{R} \quad (29b)$$

$$\forall n \in \mathcal{L}$$

$$\underline{\alpha}^n \leq K \underline{u}_{\alpha^n}, \quad \delta \circ \tau \circ D + \Delta D^n \leq K(1 - \underline{u}_{\alpha^n}) \quad (30a)$$

$$\bar{\alpha}^n \leq K \underline{u}_{\alpha^n}, \quad \delta \circ \tau \circ D - \Delta D^n \leq K(1 - \underline{u}_{\alpha^n}) \quad (30b)$$

$$\underline{\alpha}^n, \bar{\alpha}^n \geq 0, \underline{\alpha}^n, \bar{\alpha}^n \in \mathbb{R}^D, \underline{u}_{\alpha^n}, \underline{u}_{\alpha^n} \in \{0, 1\}^D \quad (30c)$$

$$\begin{aligned} \underline{u}_{\alpha^n} + \underline{u}_{\alpha^n} &\leq \varepsilon_n \mathbf{1} \\ \forall n &\in \mathcal{L} \end{aligned} \quad (30d)$$

$$\underline{\beta}^n \leq N \underline{u}_{\beta^n}, \quad M \varepsilon + S U_D \Delta D^n \leq N(1 - \underline{u}_{\beta^n}) \quad (31a)$$

$$\bar{\beta}^n \leq N \underline{u}_{\beta^n}, \quad M \varepsilon - S U_D \Delta D^n \leq N(1 - \underline{u}_{\beta^n}) \quad (31b)$$

$$\underline{\beta}^n, \bar{\beta}^n \geq 0, \underline{\beta}^n, \bar{\beta}^n \in \mathbb{R}^L, \underline{u}_{\beta^n}, \underline{u}_{\beta^n} \in \{0, 1\}^L \quad (31c)$$

$$\underline{u}_{\beta^n} + \underline{u}_{\beta^n} + \varepsilon = 1 \quad (31d)$$

$$\begin{aligned} \underline{u}_{\beta^n} &\leq \underline{u}_{\beta^n} \\ \forall n &\in \mathcal{L} \end{aligned} \quad (31e)$$

$$0 < M < N \quad (32a)$$

$$0 < K \quad (32b)$$

where λ^n is the Lagrange multiplier associated with (24). $\underline{\alpha}^n = \{\alpha_d^n\}$ and $\bar{\alpha}^n = \{\alpha_d^n\}$ are the Lagrange multiplier vectors associated with (25), whose complementary slackness conditions are represented by introducing the binary variable vectors $\underline{u}_{\alpha^n} = \{u_{\alpha_d^n}\}$ and $\underline{u}_{\alpha^n} = \{u_{\alpha_d^n}\}$, respectively. $\underline{\beta}^n = \{\beta_l^n\}$ and $\bar{\beta}^n = \{\beta_l^n\}$ are the Lagrange multiplier vectors associated with (26), whose complementary slackness conditions are represented by introducing the binary variable vectors $\underline{u}_{\beta^n} = \{u_{\beta_l^n}\}$ and $\underline{u}_{\beta^n} = \{u_{\beta_l^n}\}$, respectively. M , N , and K are sufficiently large constants.

Note that (30d) and (31e) help avoid unnecessary enumeration in the solution space and thus improve the computational performance. Note that (31d) ensures that (26) holds either

TABLE I
INTERPRETATION OF BINARY VARIABLES IN THE PROPOSED SHAPING CYBER-DEFENSE STRATEGY P2

	= 1	= 0
δ_d in (25)	no cyber-defense meter in the d -th load $-\tau_d D_d \leq \Delta D_d^n \leq \tau_d D_d$	cyber-defense meter in the d -th load $0 \leq \Delta D_d^n \leq 0$
ε_n in (26)	no cyber-defense meter in the n -th line $-M \leq S_n U_D \Delta D^n \leq M$	cyber-defense meter in the n -th line $0 \leq S_n U_D \Delta D^n \leq 0$
$u_{\alpha_d^n}$ in (30)	$\Delta D_d^n = -\delta_d \tau_d D_d$	$\Delta D_d^n \neq -\delta_d \tau_d D_d$
$u_{\alpha_d^n}$ in (30)	$\Delta D_d^n = \delta_d \tau_d D_d$	$\Delta D_d^n \neq \delta_d \tau_d D_d$
$u_{\beta_l^n}$ in (31)	$S_l U_D \Delta D^n = -M \varepsilon_n$ = 0 according to (31d)	$S_l U_D \Delta D^n \neq -M \varepsilon_n$ according to (31d)
$u_{\beta_l^n}$ in (31)	$S_l U_D \Delta D^n = M \varepsilon_n$ = 0 according to (31d)	$S_l U_D \Delta D^n \neq M \varepsilon_n$ according to (31d)

with or without line cyber-defense meters. Detailed illustrations of all binary variables are given in Table I.

Remark 1. Proposition 2 implies that protecting line measurements may not be the best decision for **P2** to reduce the maximum line overloading. Instead, to reduce the sum of the maximum line overloading of all lines, i.e., $\sum_n H_n / \bar{F}_n$ in (22), it may be more efficient to place the cyber-defense meters on loads rather than on lines. This is because a protected line measurement in **P2** only reduces the maximum overloading of the line itself, while a protected load measurement in **P2** could reduce the maximum overloading of multiple lines that are interconnected to the load bus.

B. Lower Bounds of the Big-M

There are two kinds of large constants in **P2**:

- M is introduced to set a large range for the FDI line flow injections ΔF in (26) if there exists no cyber-defense meter.
- K and N , which are also known as the big-M [19], are introduced to avoid violating the original constraints (25) and (26) when the corresponding Lagrange multipliers are not zero [20].

Inappropriate values of the big-M would deteriorate the solvability and optimum of the single-level MILP problem [20], e.g., **P2**. Specifically, too large values of M , N , and K would make the MILP problem **P2** computationally intractable, while too small values would violate the original constraints (25) and (26). Thus, closed-form lower bounds for the sufficiently large constants (M , N , and K) are addressed as follows.

Proposition 3. (Closed-Form Lower Bounds of the Big-M) M , N , and K in **P2** are sufficiently large (i.e., (25) and (26) are not violated) if

$$M \geq \| |SU_D| (\tau \circ D) \|_\infty \quad (33)$$

$$N \geq M + \| |SU_D| (\tau \circ D) \|_\infty \quad (34)$$

$$K \geq 2 \| \tau \circ D \|_\infty \quad (35)$$

Proof. See Appendix B.

C. Effectiveness and Cost-Effectiveness of the Proposed Shaping Cyber-Defense Strategy **P2**

After solving the proposed shaping cyber-defense strategy **P2**, we can obtain:

- the optimal placement of limited cyber-defense meters to minimize the FDI attack-induced region volume.
- the cyber-defense benefits with respect to a given cyber-defense cost budget \bar{C}^{AIR} .
- the cyber-defense marginal benefit with respect to the increment of the cyber-defense cost.
- the smallest number of cyber-defense meters to completely eliminate the FDI attack-induced region.

V. MAXIMIZING CYBERSECURITY MARGIN VIA A DISPATCHING CYBER-DEFENSE STRATEGY

The power system generation dispatch could be either misled by the FDI cyber-attack to achieve different attacking

purposes [11] or adopted as a powerful tool to enhance cyber resilience [21].

In particular, with limited cyber-defense resources, the proposed cyber-defense meter placement strategy **P2** may or may not completely eliminate the FDI attack-induced region Ω^{AIR} . Hence, this section proposes a cost-effective dispatching cyber-defense strategy, which achieves the trade-off between maximizing the cybersecurity margin and minimizing the additional operation costs. This is achieved by the optimal dispatch of operation points in the system operation stage.

A. Quantifying Cybersecurity Margin of Operation Points

Due to limited cyber-defense cost budget \bar{C}^{AIR} or too large cyber-defense cost coefficient ω^{AIR} , the consequent maximum line overloading (denoted as H^*) may not equal 0 after solving **P2**. In this regard, the power system still faces cyber threats from the FDI cyber-attack. Hence, a subsequent countermeasure is to dispatch the original operation point to a new one with a larger cybersecurity margin.

Considering the consequent FDI attack-induced region Ω^{AIR} (green area in Fig. 4) that is not an empty set, a subsequent countermeasure is to:

- 1) find a preventive security region (defined in Definition 5 and represented by the blue area in Fig. 4), whose boundaries are far away from Ω^{AIR} ;
- 2) find an operation point with a larger cybersecurity margin (defined in Definition 6 and represented by the circle radius in Fig. 4) inside the preventive security region;
- 3) achieve the trade-off between maximizing cybersecurity margin and minimizing additional operation costs.

Definition 4. (Preventive Line Limits) Given the consequent maximum line overloading H^* after implementing the proposed cyber-defense meter placement strategy **P2**, the preventive line limits are defined as

$$-\bar{F} + H^* \leq F = S(U_G G - U_D D) \leq \bar{F} - H^* \quad (36)$$

yielding a set of linear inequalities

$$A G \leq b \quad (37)$$

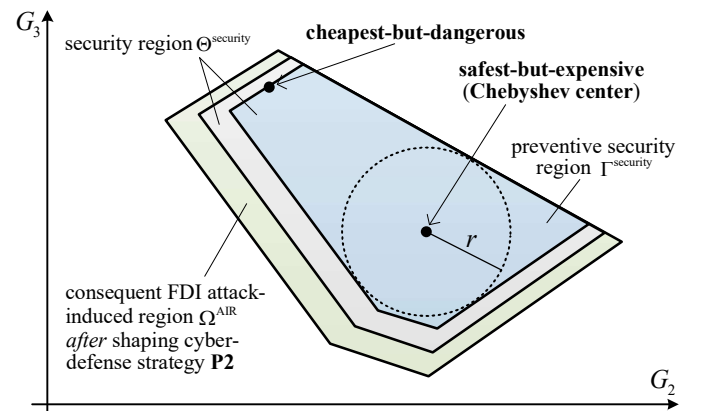


Fig. 4. Proposed dispatching cyber-defense strategy **P3** to achieve the trade-off between the safest-but-expensive operation point (i.e., the Chebyshev center) and the cheapest-but-dangerous operation point within the preventive security region

TABLE II
THE TRADE-OFF BETWEEN CYBER-DEFENSE COST AND BENEFIT OF THE PROPOSED SHAPE-AND-DISPATCH CYBER-DEFENSE STRATEGY

	shaping cyber-defense strategy P2	dispatching cyber-defense strategy P3
system stage	system planning	system operation
cyber-defense cost	number of placed meters $C^{\text{AIR}} = \sum_{d \in \mathcal{D}} (1 - \delta_d) + \sum_{n \in \mathcal{L}} (1 - \varepsilon_n)$	additional operation cost $C^G = \mathbf{c}^T \mathbf{G}$
cyber-defense benefit	opposite value of the FDI attack-induced region volume $B^{\text{AIR}} = -\sum_{n \in \mathcal{L}} H_n / \bar{F}_n$ (a measure of the set Ω^{AIR})	cybersecurity margin $B^G = r(\mathbf{G})$ (a measure of the element \mathbf{G} in the set Γ^{security})
cyber-defense decision variable	optimal meter placement on loads and lines $\delta \in \{0, 1\}^D, \varepsilon \in \{0, 1\}^L$	optimal generation dispatch $\mathbf{G} \in \mathbb{R}^G$
cyber-defense objective	trade-off between cyber-defense costs and benefits $\min -B^{\text{AIR}} + \omega^{\text{AIR}} C^{\text{AIR}}$ in (27)	trade-off between cyber-defense costs and benefits $\min -B^G + \omega^G C^G$ in (45)
information transmission	deliver the consequent maximum line-overloading \mathbf{H}^* from P2 to P3	

where

$$\mathbf{A} = \begin{bmatrix} \mathbf{S} \mathbf{U}_G \\ -\mathbf{S} \mathbf{U}_G \end{bmatrix}, \quad \mathbf{b} = \begin{bmatrix} \bar{\mathbf{F}} - \mathbf{H}^* + \mathbf{S} \mathbf{U}_D \mathbf{D} \\ \bar{\mathbf{F}} - \mathbf{H}^* - \mathbf{S} \mathbf{U}_D \mathbf{D} \end{bmatrix} \quad (38)$$

Definition 5. (Preventive Security Region) Given the consequent \mathbf{H}^* after implementing **P2**, the preventive security region is defined as

$$\Gamma^{\text{security}} := \{\mathbf{G} \mid (1), (2), (36)\} \quad (39)$$

The distance of a given operation point \mathbf{G} to the boundaries (37) is

$$q_i = \frac{|b_i - \mathbf{A}_i \mathbf{G}|}{\|\mathbf{A}_i\|_2} \quad \forall i \quad (40)$$

where \mathbf{A}_i denotes the i -th row of the matrix \mathbf{A} . b_i denotes the i -th element of the vector \mathbf{b} .

Definition 6. (Cybersecurity Margin of an Operation Point) The cybersecurity margin of a given operation point $\mathbf{G} \in \Gamma^{\text{security}}$, denoted as $r(\mathbf{G})$, is defined as the minimum Euclidean distance to the boundaries of Γ^{security} in (37).

B. Proposed Dispatching Cyber-Defense Strategy

Mathematically, the safest point (i.e., the point with the maximum security margin) inside a polytope is referred to as the Euclidean Chebyshev center [22], i.e., the center of the largest hyperball that lies inside the polytope. Thus, the safest operation point \mathbf{G} with the maximum cybersecurity margin r can be obtained by solving the linear programming problem [22]:

$$\max \quad r \quad (41)$$

$$\begin{aligned} \text{over} \quad & \mathbf{G} \in \mathbb{R}^G, r \in \mathbb{R}^+ \\ \text{s.t.} \quad & (1), (2), (37), (38) \end{aligned}$$

$$\sup_{\|\mathbf{w}\|_2 \leq r} \mathbf{A}_i(\mathbf{G} + \mathbf{w}) = \mathbf{A}_i \mathbf{G} + r \|\mathbf{A}_i\|_2 \leq b_i \quad \forall i \quad (42)$$

In this regard, the cyber-defense benefit of dispatching the operation point is defined as the cybersecurity margin:

$$B^G = r \quad (43)$$

The cyber-defense cost of dispatching is defined as the additional operation cost compared with the most economical operation point (which is a constant and thus can be omitted):

$$C^G = \mathbf{c}^T \mathbf{G} \quad (44)$$

where \mathbf{c} is the generation cost vector.

The system operators aim to maximize the cybersecurity margin and minimize the additional operation point, yielding the following linear programming problem (denoted as **P3**). This leads to a cyber-defense cost-benefit trade-off between the *safest-but-expensive* operation point (i.e., Euclidean the Chebyshev center) and the *cheapest-but-dangerous* operation point in Fig. 4.

$$\begin{aligned} \mathbf{P3} : \quad & \min_{\mathbf{G} \in \mathbb{R}^G, r \in \mathbb{R}^+} -B^G + \omega^G C^G \\ & \text{s.t. } (1), (2), (37), (38), (42), (43), (44) \end{aligned} \quad (45)$$

C. Cost-Effective Shape-and-Dispatch Cyber-Defense Strategy

As shown in Table II, the proposed cyber-defense strategy can be divided into the shaping stage and the dispatching stage, leading to a cost-effective *shape-and-dispatch* cyber-defense strategy, of which the procedure is illustrated in Algorithm 1.

Physically, the proposed shaping cyber-defense strategy **P2**, which is implemented in system planning, achieves the trade-off between minimizing the FDI attack-induced region volume and minimizing the number of cyber-defense meters via optimal meter placement. Afterwards, the consequent maximum line-overloading \mathbf{H}^* solved by **P2** is delivered to **P3** to determine the preventive security region Γ^{security} . As a result, the proposed dispatching cyber-defense strategy **P3**, which is implemented in system operation, achieves the trade-off between maximizing the cybersecurity margin and minimizing the additional operation cost via optimal generation dispatch.

Mathematically, the proposed shaping cyber-defense strategy **P2** focuses on optimizing the shape of the set Ω^{AIR} , while the proposed dispatching cyber-defense strategy **P3** focuses on finding an optimal element \mathbf{G} inside the set Γ^{security} . Note that Γ^{security} in **P3** is determined by Ω^{AIR} in **P2** via \mathbf{H}^* .

VI. CASE STUDY

To verify the effectiveness and the cost-effectiveness of the proposed cost-effective shaped-and-dispatch cyber-defense strategy, this section conducts case studies on a modified IEEE 14 bus system [23] with an additional 0.1 pu load at bus 8. The optimization problems are solved by Yalmip [24] with Gurobi [25] in a personal computer with 16 GB RAM and two 2.30 GHz processors. The power base is 100 MW.

Algorithm 1 The Proposed Cost-Effective Shape-and-Dispatch Cyber-Defense Strategy

- 1: **shaping stage:**
- 2: initialize the cyber-defense cost budget $\overline{C}^{\text{AIR}}$ and cost coefficient ω^{AIR} ;
- 3: set the lower bounds for M , N , and K according to Proposition 3;
- 4: solve the proposed cost-effective shaping cyber-defense strategy **P2** in (27);
- 5: obtain the consequent cyber-defense benefit B^{AIR} , the consequent cyber-defense cost C^{AIR} , and the optimal meter placement δ and ε .
- 6: **information transmission:** deliver the consequent maximum line-overloading H^* from the shaping stage to the dispatching stage.
- 7: **dispatching stage:**
- 8: initialize the cyber-defense cost coefficient ω^G ;
- 9: solve the proposed cost-effective dispatching cyber-defense strategy **P3** in (45);
- 10: obtain the consequent cyber-defense benefit B^G , the consequent cyber-defense cost C^G , and the optimal generation dispatch G .

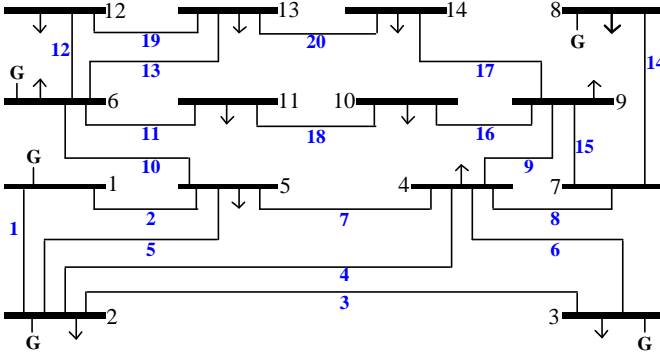


Fig. 5. A modified IEEE 14 bus systems with line indices (blue and bold) and bus indices (black)

A. Parameter Setting

As shown in Fig. 5, there are 12 loads at each bus (except for bus 1 and bus 7) and 20 lines in the modified IEEE 14 bus system [23]. To start with, we set a Base Case whose parameters are set as follows.

For the shaping stage, the cyber-defense cost budget $\overline{C}^{\text{AIR}} = 15$, indicating that at most fifteen cyber-defense meters can be deployed either in loads or in lines. The FDI cyber-attack ability is set as $\tau = 0.5$ [9], indicating the FDI cyber-attack injection at each bus is limited by 50% of the bus load. The line upper limits $\overline{F}_n = 1$ pu except for $\overline{F}_1 = 1.5$ pu. The cyber-defense cost coefficient $\omega^{\text{AIR}} = 0.15$. The sufficiently large constants $M = 1$, $N = 2$, and $K = 1$, since the lower bounds obtained from Proposition 3 are 0.9399, 1.8797, and 0.9420, respectively.

For the dispatching stage, the generation cost vector $\mathbf{c} = [20, 30, 60, 50, 25]^T$ \$/pu. The generation lower limit $\underline{G} = 0$ and upper limit $\overline{G} = 2$ pu.

B. Effectiveness of the Proposed Shaping Cyber-Defense Strategy P2

In the absence of the proposed cyber-defense meter placement strategy **P2**, the original FDI attack-induced region volume (denoted as $-B_0^{\text{AIR}} = \sum_n H_n / F_n$) solved by (8) is 2.3894 pu.

By solving **P2**, six cyber-defense meters are placed at six load measurements, whose bus indices are 2, 3, 4, 8, 9, 14, respectively. No line measurements are equipped with cyber-defense meters, which verifies Remark 1. As a result, the maximum FDI attack-induced line overloading H_n of each line is illustrated in Fig. 6. It is observed that, after implementing **P2**, H_n of each line significantly decreases. The FDI attack-induced region volume remarkably decreases by 83% (from $-B_0^{\text{AIR}} = 2.3894$ pu to $-B^{\text{AIR}} = 0.4072$ pu).

In addition, since the load at bus 8 is equipped with a cyber-defense meter, the two conditions (18) and (19) in Proposition 2 are satisfied, leading to an FDI unattackable line 14, i.e., the line from bus 7 to bus 8.

In short, the proposed shaping cyber-defense strategy **P2** successfully decreases the FDI attack-induced region volume Ω^{AIR} by optimally placing the limited cyber-defense meters.

C. Cost-Effectiveness of the Proposed Shaping Cyber-Defense Strategy P2

The proposed shaping cyber-defense strategy **P2** only adopts six cyber-defense meters instead of all fifteen cyber-defense meters, since **P2** needs to concurrently balance both the cyber-defense cost C^{AIR} and the cyber-defense benefit B^{AIR} in the objective function (27). In this regard, by varying the cyber-defense cost coefficient ω^{AIR} , the Pareto front regarding the trade-off between two cyber-defense objectives, i.e., minimizing the cyber-defense cost and maximizing the cyber-defense benefit in **P2**, is depicted in Fig. 7. For each cyber-defense cost, the corresponding cyber-defense meter placement at each load bus is depicted in Fig. 8.

It is observed that, the more expensive the cyber-defense cost (i.e., larger ω^{AIR}), the less placement the cyber-defense meters (i.e., smaller C^{AIR}). Specifically, if the cyber-defense cost is negligible (e.g., $\omega^{\text{AIR}} = 0.01$), **P2** decides to place eleven cyber-defense meters on the load buses in Fig. 8, leading to $\mathbf{H} = \mathbf{0}$ and $(B_0^{\text{AIR}} - B^{\text{AIR}}) / B_0^{\text{AIR}} = 100\%$ in Fig. 7. In other words, the system operators need at least eleven

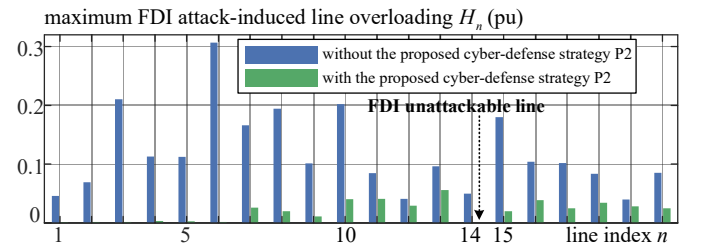


Fig. 6. Comparison of the maximum FDI attack-induced line overloading in Base Case with and without the proposed shaping cyber-defense strategy **P2**

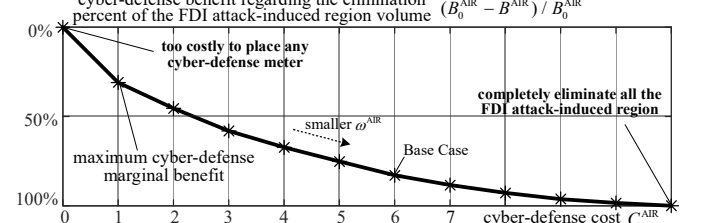


Fig. 7. Pareto front regarding the cyber-defense benefit and cyber-defense cost of the proposed shaping cyber-defense strategy **P2**

TABLE III
CONSEQUENT CYBER-DEFENSE COSTS AND BENEFITS WITH RESPECT TO DIFFERENT COST COEFFICIENTS IN THE PROPOSED DISPATCHING CYBER-DEFENSE STRATEGY **P3** AFTER IMPLEMENTING BASE CASE IN **P2**

cyber-defense cost coefficient ω^G	consequent cybersecurity margin $B^G = r$ (pu)	nearest boundaries to the operation point G	consequent cyber-defense cost $C^G = c^T G$ (\$)	generation G
0.01	1.00 (1900%) safest operation point (Chebyshev center)	$\overline{F_1}, \overline{F_3}, \overline{F_{10}}, \overline{F_{14}}, \underline{F_{14}}$	95.81 (67%) expensive operation point	$[0.38, 1.49, 0.51, 0.21, 0.10]^T$
0.015	0.84 (1580%)	$\overline{F_1}, \overline{F_3}, \overline{F_{10}}, \underline{F_{14}}$	82.87 (45%)	$[0.69, 1.40, 0.34, 0.00, 0.26]^T$
0.03	0.60 (1100%)	$\overline{F_1}, \overline{F_3}, \underline{F_{14}}$	67.20 (17%)	$[1.10, 1.09, 0.00, 0.00, 0.50]^T$
0.06	0.16 (220%)	$\overline{F_1}, \underline{F_{14}}$	58.49 (2%)	$[1.75, 0.00, 0.00, 0.00, 0.94]^T$
0.10	0.05 (0%) dangerous operation point	$\overline{F_1}$	57.25 (0%) cheapest operation point	$[2.00, 0.00, 0.00, 0.00, 0.69]^T$

cyber-defense meters to completely (100%) eliminate the FDI attack-induced region Ω^{AIR} . To avoid wasting cyber-defense resources, the rest four cyber-defense meters do not need to be placed. By contrast, if the cyber-defense cost is too expensive (e.g., $\omega^{\text{AIR}} = 1$), **P2** decides to place no cyber-defense meter.

In addition, the cyber-defense marginal benefit decreases if the cyber-defense meter increases. That is, the maximum cyber-defense marginal benefit is achieved when placing only one cyber-defense meter (at the load whose bus index is 3), which decreases the FDI attack-induced region volume by 31%.

D. Effectiveness and Cost-Effectiveness of the Proposed Dispatching Cyber-Defense Strategy **P3**

Due to limited cyber-defense cost budget $\overline{C^{\text{AIR}}}$ or too large cyber-defense cost coefficient ω^{AIR} , the FDI attack-induced region Ω^{AIR} may not be completely eliminated by the proposed shaping cyber-defense strategy **P2**, leading to $H \neq 0$. Then, the proposed dispatching cyber-defense strategy **P3** is implemented after **P2**.

By varying the cyber-defense cost coefficient ω^G , the consequent cyber-defense cost (i.e., the operation cost $C^G = c^T G$) and cyber-defense benefit (i.e., the cybersecurity margin $B^G = r$) of **P3** (after implementing Base Case in **P2**) are listed in Table III.

It is observed that a larger ω^G leads to a smaller operation cost but also a smaller cybersecurity margin. Specifically, if ω^G is large enough (e.g., $\omega^G = 0.1$), the consequent generation is $G_0 = [2, 0, 0, 0, 0.69]^T$ pu, leading to the cheapest operation cost $C^{G_0} = c^T G_0 = 57.25\$$. The minimum

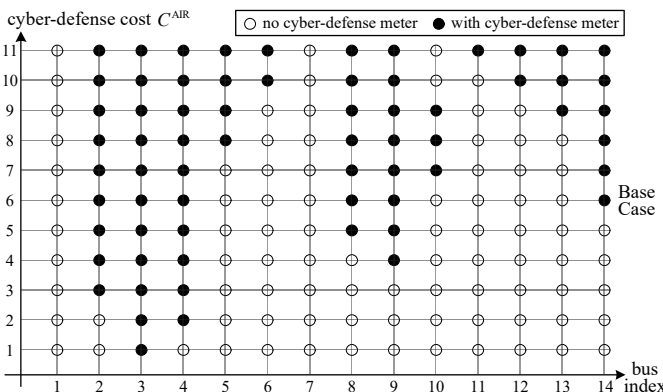


Fig. 8. Corresponding cyber-defense meter placement strategy **P2** with respect to different cyber-defense costs

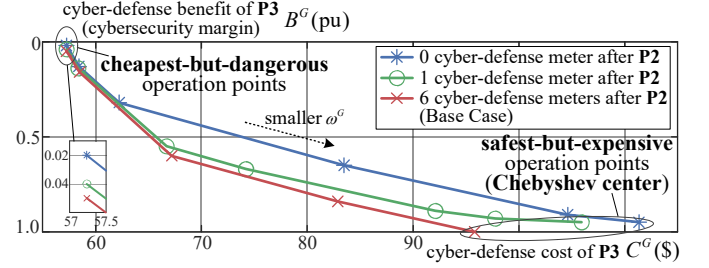


Fig. 9. Pareto front regarding the cyber-defense benefit and cost of the proposed dispatching cyber-defense strategy **P3** after different **P2** decisions

distance from the generation point G_0 to the boundaries is $q_1 = 0.05$ pu, i.e., the distance to $\overline{F_1}$. That is, the cybersecurity margin $B^{G_0} = 0.05$ pu. This leads to a *cheapest-but-dangerous* operation point.

By contrast, if ω^G is small enough (e.g., $\omega^G = 0.01$), the consequent generation $G = [0.38, 1.49, 0.51, 0.21, 0.10]^T$ pu. The operation cost is 95.81\$, which increases by 67% compared to the cheapest operation cost C^{G_0} . However, the cybersecurity margin is $B^G = r = 1$ pu, which increases by 1900% compared to $B^{G_0} = 0.05$ pu. In other words, the proposed dispatching cyber-defense strategy **P3** manages to move the cheapest-but-dangerous operation point to a *safest-but-expensive* operation point.

In addition, the cyber-defense marginal benefit decreases if the cyber-defense cost increases. The maximum cyber-defense marginal benefit is achieved if $G = [1.75, 0, 0, 0, 0.94]$, leading to 2% additional operation cost but 220% increment of cybersecurity margin.

As shown in Fig. 9, the Pareto front regarding the cyber-defense cost-benefit trade-off of **P3** is influenced by the different **P2** decisions. Although more cyber-defense meters from **P2** only slightly increase the **P3** cyber-defense benefits, the **P3** cyber-defense costs are significantly decreased when the safest-but-expensive operation points are chosen.

VII. CONCLUSION

This paper proposes a cost-effective shape-and-dispatch cyber-defense strategy against the stealthy FDI cyber-attack. First, this paper proposes a shaping cyber-defense strategy, which achieves a trade-off between shaping the FDI attack-induced region and minimizing the cyber-defense meters via optimal meter placement. Then, based on the preventive security region, this paper proposes a dispatching cyber-defense strategy, which achieves a trade-off between maximizing the

cybersecurity margin and minimizing the additional operation cost via optimal dispatch of operation points.

For the proposed shaping cyber-defense strategy in the system planning stage, the case study indicates that it optimally shapes the FDI attack-induced region with any given cyber-defense cost budget and coefficient. The optimal cyber-defense meter placement leads to an FDI unattackable line. Moreover, the smallest number of cyber-defense meters to 100% eliminate the FDI attack-induced region is identified. In addition, it is found that, using only one cyber-defense meter, the FDI attack-induced region volume is decreased by 31%, indicating the maximum cyber-defense marginal benefit.

For the proposed dispatching cyber-defense strategy in the system operation stage, the case study indicates that it successfully balances the cybersecurity margin and the additional operation cost within the preventive security region. The trade-off between the safest-but-expensive (i.e., the Chebyshev center) and the cheapest-but-dangerous operation point are addressed. In addition, it is observed that the maximum cyber-defense marginal benefit leads to 220% increment of cybersecurity margin with only 2% additional operation cost.

APPENDIX A

PROOF OF PROPOSITION 2

Proof. As shown in Fig. 10, d'_n and d''_n are the two terminal buses of the n -th line. Take bus d'_n as an example, the total FDI cyber-attack injections (except for ΔF_n) at bus d'_n is

$$\Delta P_{d'_n} = \Delta D_{d'_n} + \sum_{l \in \mathcal{N}_{d'_n}} \Delta F_l \quad (46)$$

where $\mathcal{N}_{d'_n}$ denotes the set of all lines interconnected to the bus d'_n except for the n -th line.

To satisfy one of the stealthy requirements, i.e., the power flow equation $\Delta F = SU_D \Delta D$ in (6), the FDI attack net injection at bus d'_n should be zero, yielding

$$0 = \Delta F_n + \Delta P_{d'_n} \quad (47)$$

If the cyber-defense meters satisfy $\delta_{d'_n} = 0$ in (18) and $\sum_{l \in \mathcal{N}_{d'_n}} \varepsilon_l = 0$ in (19), then both the $\Delta D_{d'_n}$ and $\Delta F_l, l \in \mathcal{N}_{d'_n}$ are disabled. Hence, we have $\Delta P_{d'_n} = 0$ and thus $\Delta F_n = 0$, leading to (17). \square

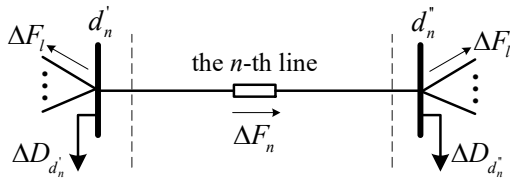


Fig. 10. The n -th line with terminal bus d'_n and d''_n

APPENDIX B

PROOF OF PROPOSITION 3

Proof. According to (26) and (25), we have

$$\begin{aligned} SU_D \Delta D &\leq |SU_D \Delta D| \leq |SU_D| |\Delta D| \\ &\leq |SU_D| (\delta \circ \tau \circ D) \leq |SU_D| (\tau \circ D) \end{aligned} \quad (48)$$

Thus, a lower bound of M in (31) is the maximum element of the vector $|SU_D| (\tau \circ D)$, yielding (33).

Similarly, according to (31), we have

$$M \pm SU_D \Delta D \leq M + |SU_D| (\tau \circ D) \quad (49)$$

Thus, a lower bound of N in (31) is the maximum element of the vector $M + |SU_D| (\tau \circ D)$, yielding (34).

According to (30) and (25), we have

$$\delta \circ \tau \circ D \pm \Delta D \leq \tau \circ D + \tau \circ D \quad (50)$$

Thus, a lower bound of K in (30) is the maximum element of the vector $2\tau \circ D$, yielding (35). \square

REFERENCES

- [1] "Power systems in transition: Challenges and opportunities ahead for electricity security," International Energy Agency, Technical Report, 2020. [Online]. Available: https://iea.blob.core.windows.net/assets/cd69028a-da78-4b47-b1bf-7520cbb20d70/Power_systems_in_transition.pdf
- [2] G. Liang, S. R. Weller, J. Zhao, F. Luo, and Z. Y. Dong, "The 2015 Ukraine blackout: Implications for false data injection attacks," *IEEE Trans. Power Syst.*, vol. 32, no. 4, pp. 3317–3318, Jul. 2017.
- [3] Y. Liu, P. Ning, and M. K. Reiter, "False data injection attacks against state estimation in electric power grids," *ACM Trans. Inf. Syst. Secur.*, vol. 14, no. 1, pp. 1–33, 2011.
- [4] A. S. Musleh, G. Chen, and Z. Y. Dong, "A survey on the detection algorithms for false data injection attacks in smart grids," *IEEE Trans. Smart Grid*, vol. 11, no. 3, pp. 2218–2234, May 2020.
- [5] D. Mukherjee, S. Ghosh, and R. K. Misra, "A novel false data injection attack formulation based on CUR low-rank decomposition method," *IEEE Trans. Smart Grid*, vol. 13, no. 6, pp. 4965–4968, Nov. 2022.
- [6] A. Abur, *Power system state estimation: theory and implementation*, ser. Power engineering ; 24. New York: Marcel Dekker, 2004.
- [7] C. Liu, M. Zhou, J. Wu, C. Long, and D. Kundur, "Financially motivated FDI on SCED in real-time electricity markets: Attacks and mitigation," *IEEE Trans. Smart Grid*, vol. 10, no. 2, pp. 1949–1959, Mar. 2019.
- [8] J. Hou, J. Wang, Y. Song, W. Sun, and Y. Hou, "Small-signal angle stability-oriented false data injection cyber-attacks on power systems," *IEEE Trans. Smart Grid*, vol. 14, no. 1, pp. 635–648, Jan. 2023.
- [9] Y. Yuan, Z. Li, and K. Ren, "Quantitative analysis of load redistribution attacks in power systems," *IEEE Trans. Parallel Distrib. Syst.*, vol. 23, no. 9, pp. 1731–1738, Sep. 2012.
- [10] L. Che, X. Liu, and Z. Li, "Mitigating false data attacks induced overloads using a corrective dispatch scheme," *IEEE Transactions on Smart Grid*, vol. 10, no. 3, pp. 3081–3091, May 2019.
- [11] Y. Yuan, Z. Li, and K. Ren, "Modeling load redistribution attacks in power systems," *IEEE Trans. Smart Grid*, vol. 2, no. 2, pp. 382–390, Jun. 2011.
- [12] L. Che, X. Liu, and Z. Li, "Fast screening of high-risk lines under false data injection attacks," *IEEE Trans. Smart Grid*, vol. 10, no. 4, pp. 4003–4014, Jul. 2019.
- [13] X. Liu, Y. Song, and Z. Li, "Dummy data attacks in power systems," *IEEE Trans. Smart Grid*, vol. 11, no. 2, pp. 1792–1795, Mar. 2020.
- [14] "Research, development & innovation roadmap 2020–2030," European Network of Transmission System Operators for Electricity (ENTSO-E), Technical Report, 2020. [Online]. Available: https://eepublicdownloads.entsoe.eu/clean-documents/Publications/RDC%20publications/entso-e-rdi_roadmap-2020-2030.pdf
- [15] E. Quah, *Cost-benefit analysis cases and materials*. Milton Park, Abingdon, Oxon :: Routledge, 2012.
- [16] P. Lau, W. Wei, L. Wang, Z. Liu, and C.-W. Ten, "A cybersecurity insurance model for power system reliability considering optimal defense resource allocation," *IEEE Trans. Smart Grid*, vol. 11, no. 5, pp. 4403–4414, Sep. 2020.
- [17] A. J. Wood, B. F. Wollenberg, and G. B. Sheblé, *Power generation, operation, and control*. John Wiley & Sons, 2013.
- [18] F. Wu and S. Kumagai, "Steady-state security regions of power systems," *IEEE Trans. Circuits Syst.*, vol. 29, no. 11, pp. 703–711, Nov. 1982.
- [19] J. Fortuny-Amat and B. McCarl, "A representation and economic interpretation of a two-level programming problem," *Journal of the Operational Research Society*, vol. 32, no. 9, pp. 783–792, 1981.

- [20] S. Pineda and J. M. Morales, "Solving linear bilevel problems using big-Ms: Not all that glitters is gold," *IEEE Trans. Power Syst.*, vol. 34, no. 3, pp. 2469–2471, May 2019.
- [21] Z. Chu, S. Lakshminarayana, B. Chaudhuri, and F. Teng, "Mitigating load-altering attacks against power grids using cyber-resilient economic dispatch," *IEEE Trans. Smart Grid*, 2022, (Early Access).
- [22] S. Boyd, S. P. Boyd, and L. Vandenberghe, *Convex optimization*. Cambridge university press, 2004.
- [23] R. D. Zimmerman, C. E. Murillo-Sánchez, and R. J. Thomas, "Matpower: Steady-state operations, planning, and analysis tools for power systems research and education," *IEEE Trans. Power Syst.*, vol. 26, no. 1, pp. 12–19, Feb. 2011.
- [24] J. Löfberg, "Yalmip : A toolbox for modeling and optimization in matlab," in *In Proceedings of the CACSD Conference*, Taipei, Taiwan, 2004.
- [25] Gurobi Optimization, LLC, "Gurobi Optimizer Reference Manual," 2023. [Online]. Available: <https://www.gurobi.com>